Proceedings RootS25
3rd International Workshop on Soil-Vegetation-Atmosphere Interaction
Boldrin D, Cecconi M, Cotecchia F, Leung A, Pedone G, Perrini P, Romero E, Tagarelli V, Zdravković L (eds)
ISSN: 3107-300X

doi: doi.org/10.53243/RootS2025-61

Shear strength at the soil-root interface under different saturation states

A. Boiero[1], E. Romero[1], M. Arroyo[1]

[1]*Universitat Politècnica de Catalunya - BarcelonaTech, and International Centre for Numerical Methods in Engineering CIMNE, Spain*

ABSTRACT: Understanding the mechanical interaction at the soil-root interface is essential for predicting how vegetation stabilises slopes, especially under changing vegetation-atmosphere conditions. One of the main challenges is the interplay between mechanical and hydraulic effects, which are mediated by soil matric suction and the degree of saturation. This study presents results from direct shear tests on representative soil-root interfaces conducted at different soil degrees of saturation and matric suctions. It considers two types of soil —silty sand and silty clay with coarse sand particles— and uses root interfaces with different surface roughness, specifically natural roots and treated wood with rough and smooth surfaces, which were characterised experimentally. The tests were performed under constant and low normal stresses (7 to 25 kPa). The ultimate shear strength reached its maximum at intermediate degrees of saturation (typically between 0.4 and 0.5), with decreases observed at both very dry (saturation 0.1) and fully saturated conditions. Natural roots consistently exhibited higher shear strength than treated wood, emphasising the importance of surface roughness.

Keywords: Soil-root interface shear strength; interface shear tests; unsaturated states; suction; bioengineering

1 INTRODUCTION

The planned application of vegetation in geotechnical engineering is generally termed bioengineering, with slope stabilisation being one of its key uses. In this context, comprehending the mechanical behaviour at the soil–root interface is crucial for assessing how vegetation contributes to slope stabilisation, particularly under variable soil–atmosphere conditions.

The mechanisms by which roots influence slope stability can be broadly classified into hydrological and mechanical reinforcement effects (Reubens et al., 2007; Giadrossich et al., 2019; among other authors). From a hydrological perspective, roots reduce soil water content through evapotranspiration—thereby increasing matric suction— and create macropores during growth, enhancing infiltration capacity at saturation. These effects operate on different timescales: infiltration is most relevant during rainfall events, whereas evapotranspiration dominates between events. On the other hand, from a mechanical perspective three root-mediated reinforcement mechanisms can be distinguished: A) basal reinforcement when crossing slip surfaces; B) lateral resistance through soil–root interface shear strength, when roots do not reach the slip surface and are located either within the sliding wedge or in the stable zone; and C) stiffen soil due to root networks within the sliding mass, mainly when interactions between neighbouring root systems occur (Reubens et al., 2007; Giadrossich et al., 2019; Boiero et al., 2024).

The root contribution in such cases is intrinsically linked to soil–root interface shear strength, which can be expressed as:

$$\tau_f = (\sigma_n - u_a)\tan\delta_{ult} + a_t \quad (1)$$

$$a_t = a' + sSr_e \tan\delta_{ult} \quad (2)$$

where τ_f is the failure interface shear strength, σ_n is the total normal stress, u_a=0 is the air pressure, a_t is the adhesion component related to soil saturation/suction conditions, a' is the minimum adhesion at null σ_n and sSr_e (associated with the non-linear behaviour of the failure envelope at low σ_n), and δ_{ult} is the ultimate friction angle at the soil-root interface. In Equation (2), s is the (matric/total) suction and Sr_e the effective degree of saturation (Romero & Vaunat, 2000; Alonso et al., 2013; Fraccica et al., 2022), which can be defined as:

$$Sr_e = \frac{Sr - Sr_m}{1 - Sr_m} \quad (3)$$

where Sr_m is a microstructural degree of saturation linked to the water stored inside aggregates. It is assumed that Sr_e can vary between 0 and 1 when Sr covers the intergranular space ($Sr_m \leq Sr \leq 1$). Equation (3) was smoothed by Gesto et al. (2011) (referred in Alonso et al., 2013) using a smoothing parameter n, to consider a small contribution when $Sr < Sr_m$:

$$Sr_e = \frac{Sr-Sr_m}{1-Sr_m} + \frac{1}{n}\ln\left[1 + e^{\left(-n\frac{Sr-Sr_m}{1-Sr_m}\right)}\right] \qquad (4)$$

From Equations (1) and (2), it follows that when soil is in contact with roots, the measured shear resistance comprises two distinct components: (i) the interface frictional contribution, related to surface roughness and interlocking; and (ii) the soil matrix stiffness contribution, controlled by the product of (total/matric) suction and the effective saturation between aggregates/particles (the effective suction or suction stress).

Root/wood surface roughness properties and soil particle size primarily determine the first component. Rough and porous surfaces (e.g. coarse roots of trees) enhance interfacial friction, while smoother surfaces (e.g. fine roots of grasses and shrubs) mainly mobilise friction without significant interlock.

The second component is mainly controlled by the soil–water retention curve (SWRC), which describes how (total/matric) suction evolves during drying or wetting and how it influences shear strength. At low degrees of saturation, the SWRC predicts high (total/matric) suctions, which can overestimate the soil matrix contribution. To address this, the effective suction (or suction stress) (sSr_e) better represents how suction is transmitted to the soil skeleton, as water action/transfer depends on the effective degree of saturation between aggregates/particles. Suction effects through menisci bridging the interface are expected at the start of the shearing stage. However, as large relative displacements occur during shearing, these menisci are broken. Therefore, it is anticipated that suction primarily affects the soil matrix, modifying the surface roughness stiffness.

Despite theoretical frameworks linking suction and surface roughness to interface shear strength, the combined influence of these factors remains poorly quantified, and experimental data remain scarce (Lin et al., 2025). This study addresses this gap by investigating soil–root interface behaviour under controlled initial degrees of saturation, which allows separating the contributions of soil matrix stiffness and interface roughness through direct shear tests.

2 MATERIALS AND METHODS

2.1 Soils

Two soils were considered in this study: material A, prepared by mixing commercial silica sand (~70%) and silt (~30%); and material B, a silty clay with coarse sand particles (finer fraction: CL) from the Llobregat river's delta (Barcelona, Spain). Their particle size distributions are presented in Figure 1, and the main physical properties are summarised in Table 1. SWRCs on wetting were determined for both materials (Figure 2). For material A, specimens were compacted at a dry state at a void ratio of e=0.645, and matric suction was monitored with a METER Group TEROS-31 tensiometer. For material B, dry samples were prepared at e=0.670, and total suction upon wetting was measured using a WP4 psychrometer, and matric suction was determined using a T5X tensiometer. Results for both soils were fitted using the van Genuchten curve (Figure 2), and the experimental sSr_e-Sr data were generated for each soil (Figure 3).

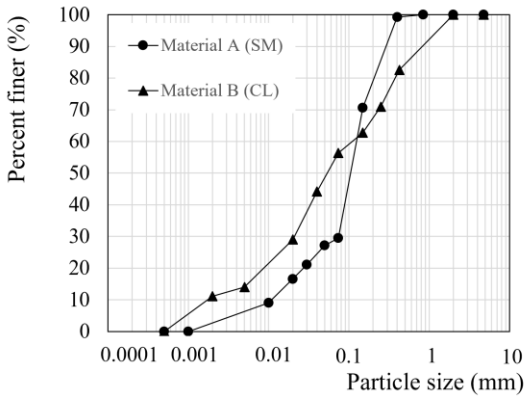

Figure 1. Soil particle distribution curves

Table 1. Physical properties of soils A and B.

	A(SM)	B(CL)
Median grain size, D_{50} (mm)	0.11	0.08
Density of solids, ρ_s (Mg/m^3)	2.65	2.70
Dry density, ρ_d (Mg/m^3)	1.61	1.68
Plastic index of finer fraction, PI	4	13
Liquid limit of finer fraction, LL	25	30
Water content (%) at RH=50%	0.30	2.11
Saturated water permeability, k_w (m/s)	5×10^{-6}	3×10^{-7}

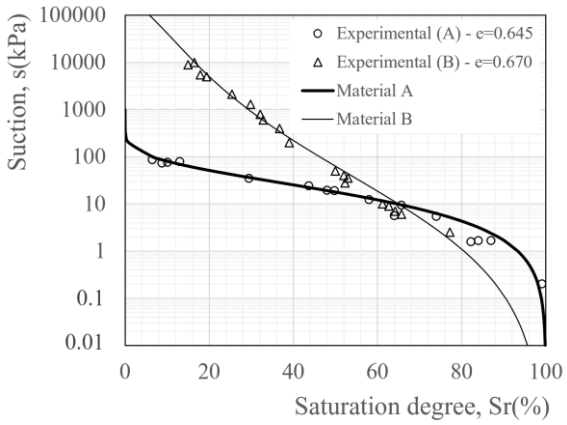

Figure 2. Experimental data and SWRC curves

Material A with low-activity fines that fill pores within a sandy skeleton causes a gradual desaturation at a relatively low air-entry value. Material B, which contains more clay, exhibits higher suctions across most of the Sr range due to increased microporosity and adsorption; however, its natural fabric includes macropores that reduce matric suction near saturation, leading to the two SWRCs crossing at Sr~65%. These differences in SWRCs are directly reflected in the effective suction response (Figure 3). Material B develops greater effective suction at an intermediate degree of saturation (around

50%) because its fine fraction generates stronger capillary and adsorptive forces. However, the presence of coarser grains (Figure 1) disrupts water continuity once saturation exceeds about 65%, thereby reducing the effective suction transmitted through the pore fluid. Conversely, the more homogeneous sand–silt matrix of material A maintains capillary connectivity over a wider saturation range, permitting higher suction stresses as full saturation is approached. This behaviour explains the intersection of both curves near Sr~65%. Sr_m values (Equation. (3)) for the different soils are indicated in the figure, which is slightly higher for soil B with a more active microstructure. The smoothing parameter (Equation. (4)) has been set at n=15 for both curves.

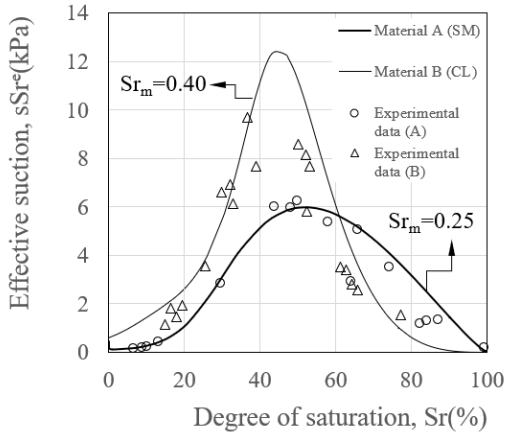

Figure 3. Curves of effective suction vs. degree of saturation

2.2 Natural roots / treated wood

Two types of wood samples were used to assess the effect of root roughness: (a) real roots of *Pinus halepensis*, from the Collserola mountain range near Barcelona (high roughness), and (b) commercially treated pine wood (low roughness). For the real root samples, the bark was carefully cut from a root approximately 120 mm in diameter into longitudinal strips about 10 mm wide and over 60 mm long. The strips were then reassembled in their original order and bonded onto an eight mm-thick wooden block, ensuring that the natural outer surface remained exposed and undisturbed within the shear zone.

Roughness was quantified using a 30-WF6207/C linear potentiometric transducer, reporting both the maximum roughness (R_t) and the average roughness (R_a). Longitudinal profiles of 60 mm were scanned at 1 mm spacing and 0.5 mm/s, following DIN EN ISO 4287. To assess how surface texture affects shear behaviour, the peak roughness R_t was scaled by the median grain size D_{50}, defining the relative roughness $R_n=R_t/D_{50}$ (Uesugi & Kishida, 1986). This nondimensional metric links root surface geometry to soil grain size and enables comparisons across materials and interfaces. Values of R_n<0.1 correspond to smooth interfaces such as steel, while R_n>1 indicates very rough surfaces with significant interlocking. In our tests, natural roots show R_n=3–4, denoting a very rough interface, whereas treated wood with R_n≈0.03 behaves as a smooth surface. Table 2 summarises the range of variability of all performed roughness measurements. The values reported in Table 2 show the contrast between natural roots and treated wood in terms of both R_a and R_t, which directly govern the mobilised friction angle and interface shear strength.

Table 2. Wood samples' roughness (range of variability)

Type	R_a (µm)	R_t (µm)	$R_n=R_t/D_{50}$ A(SM)	$R_n=R_t/D_{50}$ B(CL)
Real root	224±58	351±129	3.20±1.20	4.40±1.80
Treated wood	2.7±1.2	2.8±1.5	0.025±0.014	0.035±0.022

2.3 Direct shear apparatus setup

Interface tests were run in a Wykeham Farrance 27-WF2160 AUTOSHEAR under constant normal load conditions. Vertical and horizontal displacements were recorded with LVDTs, and shear force was measured with a 5 kN load cell using a built-in acquisition system. Matric suction was monitored with a tensiometer inserted through a 60° port in the top plate to ~5 mm above the shear band. The shear box was wrapped in plastic to limit moisture exchange with the laboratory's relative humidity.

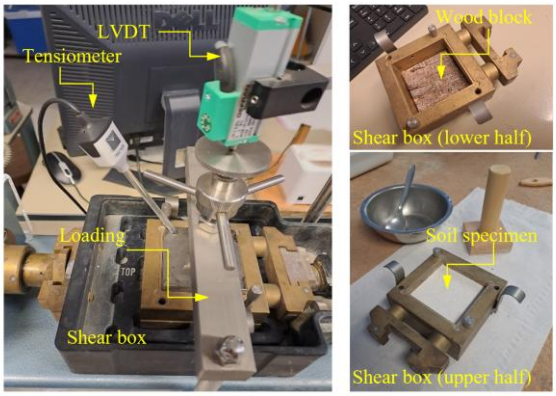

Figure 4. Direct shear box setup and sample preparation

Soil specimens were statically compacted to the target dry density and initial degree of saturation. The soil layer was 20 mm thick; a 60×60 mm dry wood block (14.5 mm high) was fixed in the lower half as the contact surface. Oven-dried soil was mixed with water to reach the target Sr, sealed for 24 h to equilibrate, and then placed to achieve the initial void ratio e_o consistent with the SWRCs. The two halves were emplaced adequately lubricated to minimise box-box friction, the target normal stress applied, and the test performed. Figure 4 shows the setup (before covering it with the plastic) and sample preparation.

3 RESULTS AND DISCUSSIONS

For the interface shear stress program, specimens of materials A and B were compacted to the same initial void

ratios used for the SWRCs. Tests spanned degrees of saturation between Sr≈0.10 and 1, under low normal stresses σ={7, 15, 25} kPa consistent with field stresses. Shearing continued to a horizontal displacement D_H=10 mm to mobilise the ultimate shear resistance (shear and normal stresses were computed using the initial area).

Figure 5 plots ultimate failure shear strengths τ_f against Sr for soil A and wood samples, including empirical fitting curves for soil-natural root interfaces. Table 3 summarises the interface parameters obtained using a minimum least-squares method. As observed, δ_{ult} values are larger for soil B, despite the more active finer fraction, and are consistent with the coarser particles and higher internal friction angle. Figure 5 indicates that natural roots consistently exhibited higher shear strength than treated wood, emphasising the importance of surface roughness (Tables 2 and 3). Figure 5 also illustrates that the ultimate shear strength reached its maximum at intermediate degrees of saturation (between Sr≈0.4−0.5 for soil A), with reductions observed at both very dry and fully saturated conditions. This trend holds at all normal stresses, with larger σ_n producing higher values.

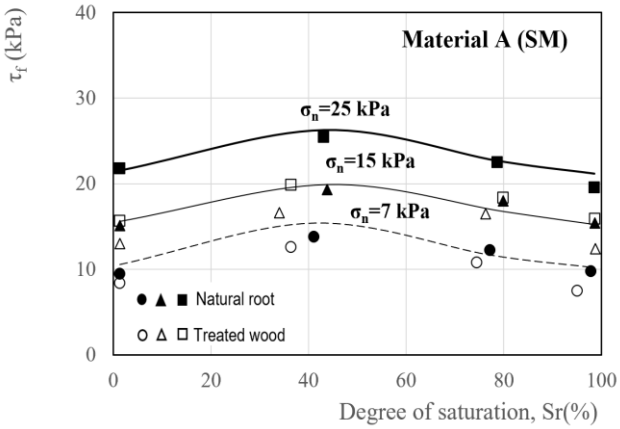

Figure 5. Variation of shear strength (τ_f) with degree of saturation (Sr) and normal stresses for material A

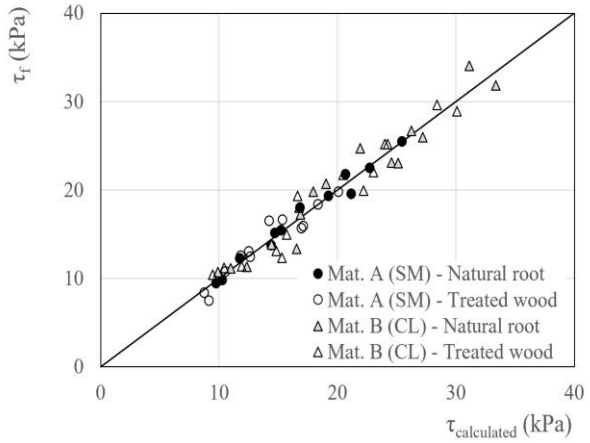

Figure 6. Experimental vs. calculated ultimate shear strengths

Figure 6 compares the experimental ultimate shear strengths (τ_f) of the studied interfaces with the corresponding estimated values ($\tau_{calculated}$) using Equations.1 to 4.

Table 3. Interface shear strength parameters.

Type	δ_{ult} (°)		a' (kPa)	
	A(SM)	B(CL)	A(SM)	B(CL)
Real root	32	41	4	4
Treated wood	26	38	4	4

4 CONCLUSION

The experimental programme emphasises the crucial roles of soil matric/total suction and root roughness in interface shear strength at ultimate conditions and highlights the importance of explicitly considering hydromechanical coupling. From a mechanical perspective, surface roughness influences interlocking and the mobilisation of the friction angle, with higher relative roughness leading to increased ultimate friction. Hydraulically, matric/total suction introduces a shear component that reaches a maximum at intermediate saturation. Their balance is strongly dependent on stress levels: suction dominates at low stresses, while mechanical friction becomes more significant as stress increases.

5 ACKNOWLEDGEMENTS

The authors are grateful for the financial support provided by MCIN/AEI/10.13039/501100011033 and Union Europea Next Generation EU/PRTR.

6 REFERENCES

Alonso, E., Pinyol, N., Gens, A. 2013. Compacted soil behavior: initial state, structure and constitutive modelling, *Géotechnique* **63**, No. 6, 463-478.

Fraccica A., Romero, E., and Fourcaud, T. 2022. Tensile strength of a compacted vegetated soil: Laboratory results and reinforcement interpretation, *Geomechanics for Energy and the Environment* **30**, 100303.

Giadrossich, F., Cohen, D., Schwarz, M., Ganga, A., Marrosu, R., Pirastru, M., Capra, G. 2019. Large roots dominate the contribution of trees to slope stability, *Earth Surf. Process. Landforms* **44**, 1602-1609.

Lin, Y., Jian, W., Wu, Y., Zhu, Z., Wang, H., Dou, H. Fan, X. 2025. Degradation of the mechanical properties of root-soil composites under moisture influence, *Bulletin of Engineering Geology and the Environment* **84,**160.

Reubens, B., Poesen, J., Danjon, F., Geudens, G., Muys, B. 2007. The role of fine and coarse roots in shallow slope stability and soil erosion control with focus on root system architecture: a review, *Trees* **21**:385-402.

Romero, E., Vaunat, J. 2000. Retention curves on deformable clays. *Experimental Evidence and Theoretical Approaches in Unsaturated Soils* (Eds: Tarantino, A. & Mancuso, C.). Balkema, Rotterdam. ISBN 90 5809 1864.

Uesugi, M., Kishida, H. 1986. Frictional resistance at yield between dry sand and mild steel, *Soils and Foundations* **26**(4), 139-149.